A&A manuscript no.
(will be inserted by hand later)

Your thesaurus codes are:
4(8.11.1; 10.06.2; 10.11.1; 10.19.1; 10.19.3)

ASTRONOMY
AND
ASTROPHYSICS
1.2.2008

Stellar kinematics in the solar neighbourhood and the disc scale lengths of the Galaxy

O. Bienaymé and N. Séchaud

Observatoire de Strasbourg, CNRS URA 1280, 11 rue de l'Université, F-67000 Strasbourg, France

Received 7 May 1996, accepted January 1997

Abstract. A general dynamically consistent 2D flat distribution function is built to model the kinematics of neighbouring stars. Application leads to the measurement of a short galactic scale length R_ρ between 1.7 and 2.9 kpc and a locally decreasing rotation curve. This is in agreement with recent determinations based on kinematics and counts of distant stars. These results rule out the classical assumption that $2R_\rho = R_\sigma$ or that $\sigma_z(R)/\sigma_R(R)$ is constant when the vertical scale height $h_z(R)$ is assumed to be constant. We explain why the measured squared axis ratio of the velocity dispersions σ_v^2/σ_u^2 of disc stars is less than 1/2. This ratio has been claimed to be important evidence for the non-axisymmetry of the galactic disc. We show that this is not the case and that it may be simply explained with a realistic axisymmetric disc model if the circular velocity is locally declining or if there is a mismatch between the photometric and kinematic scale lengths.

Key words: Stars: kinematics – Galaxy: kinematics and dynamics – solar neighbourhood – Galaxy: structure –

1. Introduction

Dynamical self-consistent constraints deduced from the Boltzmann equation are necessary to analyse and interpret kinematic data in the Galaxy. It has been shown that the standard epicycle theory approach, a first order theory to estimate galactic characteristics, is subject to systematic errors (see Kuijken & Tremaine 1991, who put forward higher order developments). In some recent work, distribution function solutions of the Boltzmann equation (proposed by Shu 1969) and/or third moments in Jeans equations (Cuddeford & Amendt 1991) have been used to obtain a more consistent description of our Galaxy (Cuddeford & Binney 1994, Kuijken & Tremaine 1991, Evans & Collett 1993, Fux & Martinet 1994). With different approaches, they attempt to determine and to make use of exact constraints between global parameters describing our Galaxy, namely the slope of the circular velocity curve, the density and kinematic scale lengths etc...

In this paper, we give a short review of observational constraints and the different values taken by these authors. Secondly we build a new model of Shu-type distribution functions where scale lengths and the shape of the velocity curve are free parameters. Thirdly we compare and adjust this model to velocity distributions of stars in the solar neighbourhood taken from the Gliese catalogue and other catalogues. Implicit constraints are related to the asymmetric drift relation and the Lindblad equation that gives the ratio of radial and tangential velocity dispersions. We conclude that extended Shu distribution functions recover most of the fundamental kinematic properties of the galactic disc. We show that it is possible to build a consistent model explaining local stellar kinematics and to determine local structural galactic parameters.

Send offprint requests to: O.Bienaymé

2. Observational constraints

We use local kinematic data from Gliese & Jahreiss (1991) and other catalogues to constrain galactic structure. Stars near the sun with large relative velocity provide information on non-local galactic structure like the kinematic and density gradients or the slope of the rotation curve. The local star velocity distribution is a section of phase space and this observed distribution depends on non-local quantities like the potential, or global density distribution of stars (other examples are given by Dehnen and Binney 1995, who describe ways to map the Galaxy's gravitational potential and distribution of matter). We show that the analysis of local kinematics is able to recover the potential gradient and stellar scale lengths. In previous analyses, assumptions have been either a flat velocity curve (Evans & Collett 1993) or a relation between density and kinematic gradients (Cuddeford & Binney 1994). These assumptions allow these authors to obtain tractable distribution functions. However they found that these distribution functions are not compatible with existing observational evidence. We discuss observational evidence on galactic structure, and emphasize the existing systematic differences between authors.

2.1. The circular velocity curve

Determinations of the galactic circular velocity curve are based on radial velocity observations of objects belonging to the disk population. Due to their small velocity dispersion, they follow the galactic rotation curve closely. However exact determination of the velocity curve depends critically on the adopted galactic radius R_0 and circular velocity Θ_0 at the solar position. Assuming $R_0 = 7.9\,\mathrm{kpc}$ and $\Theta_0 = 185\,\mathrm{km\,s^{-1}}$, Rohlfs and Kreitschmann (1988) found that the velocity curve "is slowly declining from $\Theta = 200\,\mathrm{km\,s^{-1}}$ at $R = 4.5\,\mathrm{kpc}$ to $\Theta = 173\,\mathrm{km\,s^{-1}}$ at $R = 11\,\mathrm{kpc}$" (however taking $\Theta_0 = 220\,\mathrm{km\,s^{-1}}$, they obtained a flat rotation curve). This result is also corroborated by Fich et al. (1989), Pont et al. (1994) and by Dambis et al. (1995).

Since most recent determinations favor values around $R_0 = 7.9\,\mathrm{kpc}$ (Reid 1993) or $R_0 = 8.1\,\mathrm{kpc}$ (Pont et al. 1994) and $\Theta_0 = 185\,\mathrm{km\,s^{-1}}$, much smaller than the recommended values of $R_0 = 8.5\,\mathrm{kpc}$ and $\Theta_0 = 220\,\mathrm{km\,s^{-1}}$ by the IAU general assembly in 1985 (Kerr & Lynden-Bell 1986), we consider it very likely that the circular velocity curve is locally declining. We estimate $\alpha \simeq -0.1$ to -0.3 for $v_c(R) = R^\alpha$ at the solar galactic radius of $R_0 = 7.5\,\mathrm{kpc}$ and $\Theta_0 = 185\,\mathrm{km\,s^{-1}}$.

Considering the Lindblad equation $\sigma_\phi^2/\sigma_R^2 \simeq \frac{1}{2}(1 + \frac{d\ln\ v(R)}{d\ln R})$, we conclude that there is no a priori conflict between the slope of the rotation curve and the observed ratio of velocity dispersion σ_ϕ^2/σ_R^2 smaller than $\frac{1}{2}$ (Kerr & Lynden-Bell 1986).

2.2. The disc density scale length

Most disc density scale length determinations range between 2.5 and 5 kpc (see Kent et al. 1991 and Robin et al. 1992a), but part of these measurements are model dependent and require assumptions. Assuming $\sigma_R(R) = \exp(-R/2h)$, Lewis & Freeman (1989) gave $h = 4.4\,\mathrm{kpc}$ from velocity dispersions of distant K giants. van der Kruit (1986) obtained a larger value of 5.5 kpc from the *Pioneer* 10 background experiment. But his determination gives access only to the radial to vertical scale ratio, and he assumed a $h_z = 325\ pc$ vertical scale height for the old disc. Adopting the recent determination of 250 pc for h_z (Kuijken & Gilmore 1989, Haywood et al. 1996), the radial scale length deduced from *Pioneer* 10 data would be closer to 4.2 kpc. Recent direct determinations range between 2.5 kpc (star counts: Robin et al. 1992ab, Ojha et al. 1996, COBE map: Durand et al. 1996) and about 3.5 kpc (Kent et al. 1991). We note that the kinematic determination of the radial scale length obtained by Fux & Martinet (1994) is $h = 2.5\,\mathrm{kpc}$, assuming a radially constant scale height h_z, and $h = 3.1\,\mathrm{kpc}$ with a positive local h_z gradient of $30\,pc/\mathrm{kpc}$. Their analysis is based on the asymmetric drift equation and on moments of the Boltzmann equation.

2.3. The disc kinematic scale length

We know only few direct determinations for the kinematic scale length of stellar discs in the Milky Way. Neese & Yoss (1988) measured the gradient of radial velocity dispersion from 364 stars mainly towards the galactic anticentre and found $\partial\sigma_R/\partial R = -3.8 \pm 0.6\,\mathrm{km\,s^{-1}\,kpc^{-1}}$ or $\partial \ln \sigma_R^2/\partial R = -(3.7\,\mathrm{kpc})^{-1}$. Lewis & Freeman (1989) obtained 4.4 kpc for the σ_R^2 scale length (or 8.8 kpc for σ_R). These results are based on 600 distant giants towards the galactic centre and anticentre. As remarked by Evans & Collett (1993), the Lewis & Freeman (1989) fit is probably not good at the solar position and a different value for the velocity dispersion at the solar galactic radius based on K giants (Delhaye 1965) should be used. With this value Evans & Collett (1993) tried a non-exponential function to model the radial dependence of velocity dispersions and obtained a better fit. Using this function, we obtain for the local kinematic scale length $\partial \ln \sigma_R^2/\partial R = (-4.8\,\mathrm{kpc})^{-1} = -0.21\,\mathrm{kpc^{-1}}$. This illustrates the precision of the determination. From

star counts and proper motions Ojha et al. (1996) measured velocity dispersion and gradients and obtained similar kinematic scale lengths.

It is usually accepted that galactic discs have constant scale heights and exponentially decreasing velocity dispersions. Measured velocity dispersions in galactic discs led Bottema (1993) to conclude that the velocity dispersion decreases exponentially with radius like $\sigma_R^2 \sim e^{-R/R_\rho}$ if the vertical to radial velocity dispersion ratio is constant with radius. This last current assumption (or the plane-parallel assumption) must be ruled out if, for example, the observations in the Milky Way show that $R_\rho \neq R_{\sigma^2}$.

For a given disc galaxy, there is not a strong chromatic dependence of the scale length (Elmegreen & Elmegreen 1984, Giovanardi & Hunt 1988). The bulk of 86 spiral galaxies (Fig. 9 by de Jong, 1996) shows $R_B/R_K \sim 1.2$. This is a strong indication that the stellar populations are distributed in discs with similar scale lengths. For our model fitting in the next section, we will assume no chromatic dependence for our Galaxy. We will assume the same for kinematic scale lengths though there are no existing observations that confirm this.

2.4. Disc axisymmetry

Evidence from a variety of sources shows the existence of a bar in the central few kpcs of the galactic center, with rough agreement on the orientation of the bar. However it is much more difficult to find evidence from star counts in the galactic plane for ellipticity of the stellar disc at the solar galactic radius, particularly if we are on one of the symmetry axes.

Signatures from kinematics give more reliable constraints (Kuijken & Tremaine 1994): 1) Oort's constants C and K and the LSR radial velocity show no evidence for local non-axisymmetry, 2) while vertex deviation for low velocity dispersion and young stars may show such evidence this last effect could be caused by very local non-stationary effects related to the presence of spiral arms, 3) for stars in the solar neighbourhood of high velocity dispersion, the velocity ellipsoid points towards the galactic centre ($l = 5.5^\circ \pm 4.2$), with no indication of local non-axisymmetry, 4) the axis ratio σ_v/σ_u is observed to be about ~ 0.5 and can be a signature of ellipticity but as we show in detail in this paper, it may also be explained if the rotation curve is locally decreasing or if the kinematic and density scale lengths are very different.

Stronger arguments in favour of the effect of a bar at $R = R_0$ come from the Blitz & Spergel (1991) analysis of HI data from which they deduced that the LSR has a radial motion of $14\,\mathrm{km\,s^{-1}}$. However the effect of the warp beyond $R = 12\,\mathrm{kpc}$ (Burton & te Lintel Hekkert 1986) may modify their analysis and the LSR radial motion is not confirmed by other observational measurements: $v_r(LSR) = -1 \pm 9\,\mathrm{km\,s^{-1}}$ (Table 3 in Kuijken & Tremaine 1994). As a conservative hypothesis we will still assume that the galactic disc is axisymmetric and we will show that local kinematics may be explained in the frame of this hypothesis.

2.5. The vertical structure

A plane-parallel potential is developed in the next section. Such potentials do not permit the consideration of the correlations between vertical and radial motions that must exist. From the probable mass galactic distribution, these correlations have certainly a better representation with a spherical potential than with a plane-parallel one (this is not true for the density distribution). Such a spherical potential will be briefly developed in the next section and general solutions fitting observational constraints will be given in Section 4. Intermediate galactic potentials between plane parallel and spherical do not have 3 known integrals of motion (with the exception of Stäckel potentials) and cannot be used to find simple analytic distribution functions. For this reason we restrict the present analysis to Stäckel potentials to include the effect of the vertical structure. In these cases, the distribution functions are deduced following Statler (1989) and are extensions of the Shu and Schwarzschild distribution functions.

Vertical structure introduces a bias on the Lindblad and asymmetric drift equations which is estimated by Cuddeford & Binney (1994). The complete analysis done by Fux and Martinet (1994) allows them to measure locally the third order derivative term of the potential related to the flatness of the potential. This derivative is related to the radial gradient of the vertical scale height h_z.

3. Galactic disc distribution function

Shu (1969) described a phenomenological distribution function (DF) that has the great advantage of relative simplicity and that has been used frequently. This distribution function is a two dimensional representation of a flat and rapidly rotating stellar disc in an axisymmetric potential (rotational symmetry). The DF is written explicitly in terms of two integrals of motion (energy and angular momentum) and is a steady-state solution of the Boltzmann equation if the potential is time-independent. For small velocity dispersions, Shu's DF closely approximates the Schwarzschild

velocity ellipsoid DF. Two functions are free: the input surface density distribution $\widetilde{\Sigma}(R)$ and the input radial velocity dispersion $\widetilde{\sigma}(R)$ (Shu 1969, Tamisier 1991). The main advantage of the Shu DF is that the associated exact surface density distribution $\Sigma(R)$ and radial velocity dispersion $\sigma_R(R)$ (DF moments of 0 and 2^{nd} order) will in general remain close to the input functions $\widetilde{\Sigma}(R)$ and $\widetilde{\sigma}(R)$, even with quite large velocity dispersions. We define the Shu DF as

$$f\left(E,L_z\right)=\frac{2\Omega\left(R_c\right)}{\kappa\left(R_c\right)}\frac{\widetilde{\Sigma}\left(R_c\right)}{2\pi\widetilde{\sigma}^2\left(R_c\right)}\exp[-\frac{\left(E-E_{circ}\left(R_c\right)\right)}{\widetilde{\sigma}^2\left(R_c\right)}]\quad\text{if}\quad L_z>0 \tag{1}$$

$$f(E,L_z)=0\quad\text{if}\quad L_z\leq 0, \tag{2}$$

where $R_c=R_c(L_z)$ is the radius of the circular orbit with angular momentum L_z, ($R_c(L_z)$ is bijective for potentials considered in the next sections), $E_{circ}(R_c)$ is the energy of a circular orbiting star at radius R_c with angular momentum L_z. Ω is the angular velocity and κ is the epicyclic frequency $2\Omega[1+\frac{1}{2}d\ \ln\Omega/d\ \ln\ R]^{1/2}$. The exponential part of the DF (Eq.1) represents a ring of stars with angular momentum L_z rotating near the radius R_c and with radial velocity dispersion $\widetilde{\sigma}$. The other terms are normalizations which permit a distribution of elementary rings with different L_z (and R_c) and with a total mean density close to $\widetilde{\Sigma}(R)$. Equation 2 is given to ensure that the total angular momentum of the disc is non-zero. In this model the disc has a maximum rotation compared to any other distribution function with the same resulting density and no retrograde orbits are allowed. Here these restrictions have no consequence since we analyse the local kinematics where only one retrograde orbit is found among one thousand stars.

Since we want to build a model whose resulting density is $\Sigma(R)\sim\Sigma_0\exp(-R/R_\rho)$, we put

$$\widetilde{\Sigma}(R_c(L_z))=\Sigma_0\exp[-R_c(L_z)/R_\rho] \tag{3}$$

and in order to have a nearly exponential $\sigma_R(R)$ distribution, we put

$$\widetilde{\sigma}(R_c(L_z))=\sigma_0\exp[-R_c(L_z)/R_\sigma]. \tag{4}$$

Thus the DF depends only on the integrals of motion and on the following free quantities: the velocity curve $v_c(R)$ and the two constant scale lengths R_ρ and R_σ.

3.1. Flat rotation curve model

We describe a model with a flat rotation curve $v_c(R)=1$ and a potential given by $\Phi(R)=\ln(R)$. Then we have $R_c(L_z)=L_z/v_c(R_c)=L_z$. Pertinent parameters are the amplitude σ_0 and the scale length ratio R_σ/R_ρ. We define models with quasi-exponential density and dispersion distributions:

$$\widetilde{\Sigma}(R_c(L_z))=\Sigma_0\exp[-L_z/R_\rho] \tag{5}$$

and

$$\widetilde{\sigma}(R_c(L_z))=\sigma_0\exp[-L_z/R_\sigma]. \tag{6}$$

For different values of σ_0, Figs. 1a-2a show that the density $\Sigma(R)$ and the radial velocity dispersion $\sigma_R(R)$ remain close to an exponential (with scale lengths R_ρ and R_σ respectively) for models with the smallest velocity dispersions. For the largest dispersion ($\sigma_0=.64$), the effective density scale length is larger than the R_ρ parameter. The mean streaming velocity $\overline{v}_\phi$ (Figs. 1b-2b) of the modelled stellar populations departs from the circular velocity curve ($v_c(R)=1$). This is due to asymmetric drift which is directly related to the amplitude of the radial velocity dispersion. For the models with large σ_0, the ratio σ_ϕ/σ_R (Figs. 1c-2c) departs from the limiting value $\sqrt{2}/2$ for zero velocity dispersion.

These results can be directly compared to that of Evans & Collett (1993) and Cuddeford & Binney (1992): the velocity dispersion ratio can be much smaller than $\sqrt{2}/2$, as observed in the solar neighbourhood (Table 8 of Kerr & Lynden-Bell 1986) in at least three situations: R_0 is smaller than R_ρ, R_σ is much larger than R_ρ or the rotation curve is decreasing with radius.

For small velocity dispersions, the ratio σ_ϕ/σ_R depends only on the shape of the velocity curve. This is not true for large dispersions, where dependence on the scale lengths is significant.

Shu-type models exist with the Lewis & Freeman (1989) assumption that $2R_\rho=R_\sigma$ (Fig. 1), (see for example Binney 1987, Kuijken & Tremaine 1991 and Cuddeford & Binney 1992). Such models imply that $R_\rho>5\,\mathrm{kpc}$ (i.e. $R_0/R_\rho<1.6$) to explain measured ratios σ_ϕ/σ_R smaller than $\sqrt{2}/2$. It may be also accounted for if $R_\sigma/R_\rho>>2$ (Fig. 2).

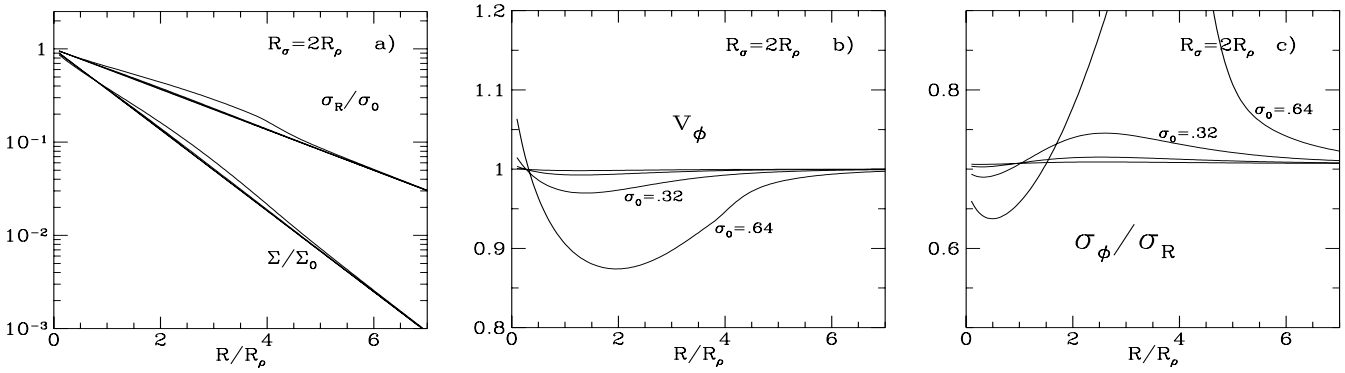

Fig. 1. (a) The surface density $\Sigma(R)$ and the radial velocity dispersion $\sigma_R(R)$ generated in a logarithmic potential by the distribution of Eqs. 1, 7 and 8 with $R_\sigma = 2R_\rho$ and four different σ_0 =(.08,.16,.32,.64). (b) The mean streaming velocity. (c) The velocity dispersion ratio.

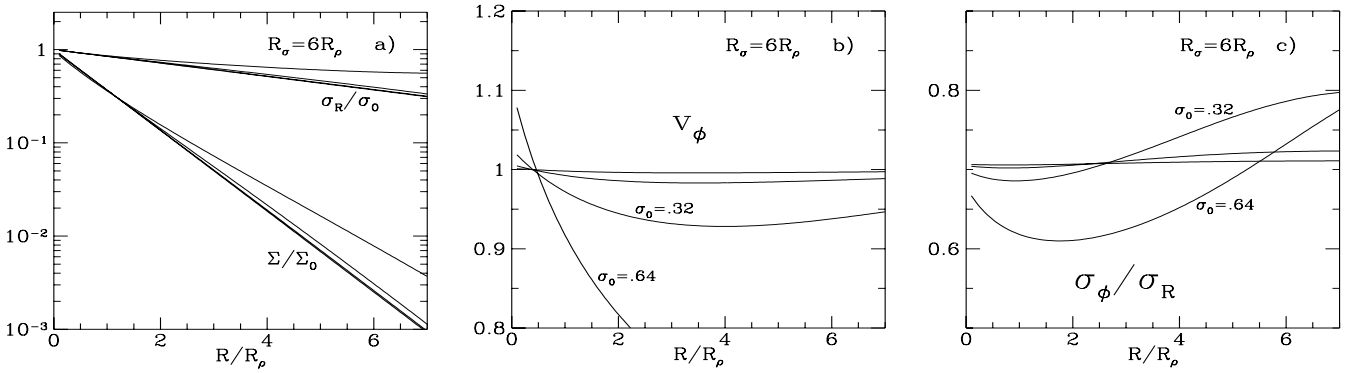

Fig. 2. Same as Figure 1, but with $R_\sigma = 6R_\rho$. (a) Surface density and radial velocity dispersion. (b) The mean streaming velocity. (c) The velocity dispersion ratio.

3.2. Power law rotation curve models

In what follows we use a more general model with potentials yielding a power law circular velocity curve: $v_c(R) = R^\alpha$. The radius of a circular orbit with momentum L_z is given by $R_c(L_z) = L_z/v_c = L_z^{\frac{1}{\alpha+1}}$ and the circular velocity is $v_c(L_z) = L_z^{\frac{\alpha}{\alpha+1}}$. This gives for $\widetilde{\Sigma}$ and $\widetilde{\sigma}$:

$$\widetilde{\Sigma}(L_z) = \Sigma_0 \exp[-L_z^{\frac{1}{\alpha+1}}/R_\rho] \tag{7}$$

$$\widetilde{\sigma}(L_z) = \sigma_0 \exp[-L_z^{\frac{1}{\alpha+1}}/R_\sigma] \tag{8}$$

Here again the resulting density and dispersion will be in general nearly exponential with scale lengths R_ρ and R_σ, but models loose this convenient behaviour when the velocity dispersions are too high.

Other Shu models could be built using different closed forms or using some spline functions to fit data obtained along the galactic radius. Such phenomenological models are certainly less elegant than for example Evans & Collett (1993) exact models that give DFs for a few defined density or dispersion distributions. However Shu models are more flexible, cover a larger range of model types and they have a sufficient number of free parameters for basic comparison to observations. Thus they allow a more extensive comparison to available data.

3.3. 3D models

3D models are built to include the vertical structure of the potential. We detail two cases for which explicit DFs are easy to obtain. In the case of a plane parallel potential, the DF may be multiplied by the trivial term:

$$\frac{1}{(2\pi)^{1/2}}\frac{1}{\widetilde{\sigma_z}(L_z)}exp^{-\frac{\dot{z}^2}{2\sigma_z^2}} \quad . \tag{9}$$

For a spherical potential, a 3 dimensional DF may be deduced from the DF given by Equ. (1) and from the equation 11b given by Statler (1989) for Stäckel potentials; in the case of a flat rotation curve, the vertical term is:

$$\frac{1}{(2\pi)^{1/2}}\frac{1}{\widetilde{\sigma_z}(L_z)}exp^{-\frac{\dot{z}^2}{2}\left[\frac{1}{\sigma^2}+(\frac{1}{\sigma_z^2}-\frac{1}{\sigma^2})\frac{v_\phi^2}{v^2}\right]} \quad . \tag{10}$$

This shows that the correlation term is the most different for the highest velocity dispersion populations. In the next section we consider plane parallel and spherical models with power law rotation curves. Other more general models using DFs in Stäckel potentials (Statler 1989) have also been used to examine solutions in intermediate potentials between plane-parallel and spherical ones. In the present context DFs in Stäckel potentials introduce a new parameter: the focus of the ellipsoidal system of coordinates (Statler, 1989). For all these models we have assumed that the (radial) vertical and (radial) horizontal dispersion kinematic scale lengths are equal $R_{\sigma_z} = R_\sigma$. The results of these intermediate models are presented in Section 4.3 and can be compared to the plane-paralel model solutions.

4. Models versus Observations

4.1. Observational data

In this section we compare the models presented in the previous section to the local stellar kinematics as given by two catalogues. The first one is the recently published Reid et al. (1995) catalogue that improves considerably the data for K and M stars found in the CNS3 catalogue of nearby stars (Gliese & Jahreiss 1991). They include new radial velocity measurements and reject stars with incorrect spectral types or giants previously misclassified as dwarfs.

We build a second catalogue by extending as much as possible the CNS3 catalogue using the Simbad database at the CDS in Strasbourg and by completing missing data, colours, radial velocities and some trigonometric parallaxes when new observations are available (mainly from the Hipparcos Input Catalogue, Turon et al. 1992) but also from a bibliography of radial velocities (Barbier-Brossat et al. 1994) and the General Catalogue of Trigonometric Stellar Parallaxes (Van Altena et al. 1991). We remove misclassified stars identified by Reid and stars with $M_v > 8$. We retain only O to G type stars to get a catalogue complementary to Reid's catalogue.

We extract from these catalogues distance-limited samples in order to obtain homogeneous and kinematically unbiased 3D velocity distributions. We use distance criteria given by Reid et al. (1995) for their catalogue, and apply a similar process to define the completeness limits for the second catalogue (26 pc for $M_v < 3$, 23 pc for $3 < M_v < 5$ and 21 pc for $5 < M_v < 8$).

Finally we consider multiple stars as one kinematic object since the kinematics of the members are correlated. We reject one star with a velocity modulus larger than 200 km s^{-1} that is certainly a halo star unmodelled by our DF.

Stars or data not in the CNS3 and Reid catalogues are given in Tables 1 and 2.

4.2. Model adjustment

Distribution functions are modeled by Eqs. 1, 2, 7 and 8. Data-model comparison is done by adjustment of model parameters using the maximum likelihood method in the (v_R, v_ϕ) space for plane-parallel models (and v_R, v_ϕ, v_z for 3D models). All stars are assumed to be at solar galactic radius $R = R_0$. The $u_\odot$, $v_\odot$ components of the solar velocity relative to the LSR are two local parameters. Other parameters Σ_0, σ_0 are dependent upon the local number of stars and the local radial velocity dispersions. Non-local parameters are the kinematic and the density scale lengths of stellar populations and the slope of the circular velocity curve. These quantities are obtained as a mean over a few kiloparsecs around the solar galactic radius corresponding to the extent of the radial excursions of stars that are in the solar neighbourhood, and that collectively carry some information from these more distant regions. For 3D models, the coordinate of the focus of the ellipsoidal coordinate system used to define the Stäckel potential is a supplementary adjustable parameter.

The radial to tangential velocity dispersion ratio of a low dispersion population constrains mainly the slope of the circular velocity curve. For kinematically hot populations, this ratio depends also on R_ρ and R_σ. The mean velocity

Table 1. Stars with new measurements labelled with *. Other data are taken from the CNS3. New V_{rad} are extracted from Barbier-Brossat et al. (1994), trigonometric parallaxes from the General Catalogue of Trigonometric Stellar Parallaxes (Van Altena et al. 1991) and B-V from the Hipparcos Input Catalog (Turon et al. 1992).

Identification number	α_{1950}	δ_{1950}	$15\mu_\alpha \cos\delta$ $''/y$	μ_δ $''/y$	V_{rad} km.s^{-1}	Sp	M_v	B-V	π mas	u	v km.s^{-1}	w
HD 8357	01 20 20	07 09.3	0.095	0.239	0.0*	G5	6.43		66.0	-13	8	11
Gl 174.1A	04 38 57	-41 57.5	-0.198	-0.076	-0.6*	F2 V	2.70	0.34	44.8	11	7	-11
HD 30090	04 42 56	42 15.5	0.000	0.065	28.8	G0	5.10	0.70*	52.0	-26	13	3
HD 38114	05 41 35	32 22.3	0.020	-0.083	-44.4*	G5	6.56		48.0	44	-10	-4
Gl 244 A	06 42 57	-16 38.8	-0.570	-1.210	-7.6*	A1 V	1.47	0.00	380.4	14	0	-11
Gl 253	06 53 51	-55 11.5	-0.042	-0.180	40.1	G7 V	7.38	0.78	69.6*	8	-36	-20
Gl 274 A	07 25 54	31 53.1	0.181	0.173	-4.4*	F0 V	3.04	0.32	59.1	9	10	14
Gl 291 A	07 49 27	-13 45.8	-0.069	-0.344	-17.8*	F9 V	4.71	0.57	62.7	25	0	-19
Gl 292.2	07 52 03	-01 16.8	-0.278	-0.054	93.4*	G8 V	5.60	0.73	51.9	-77	-58	-2
HD 108081	12 22 25	-03 56.7	-0.144	-0.214	47.0	G5	6.80	0.66*	54.7	7	-43	29
HD 163621	17 53 40	36 11.7	-0.145	-0.015	0.0*	G5	6.33		50.0	2	-6	9

Table 2. Supplementary stars. Data obtained or deduced from the Hipparcos Input Catalog (Turon et al. 1992).

HIC number	α_{1950}	δ_{1950}	$15\mu_\alpha \cos\delta$ $''/y$	μ_δ $''/y$	V_{rad} km.s^{-1}	Sp	M_v	B-V	π mas	u	v km.s^{-1}	w
3405	00 41 07	-57 44.2	-0.012	0.011	2.0	A0 IV	2.36	0.02	39.0	1	1	-2
4422	00 53 40	58 54.7	-0.174	-0.048	-47.6	G8 IV	2.64	0.96	40.0	35	-34	-3
6607	01 22 27	-28 05.7	0.359	-0.287	87.2	G6 V	7.46	0.68	68.0	-14	-36	-83
9381	01 58 25	-40 58.0	0.593	-0.436	-27.5	G3 V	5.99	0.65	53.0	-1	-43	45
20347	04 19 27	-25 50.7	0.056	-0.056	18.0	F2 V	4.48	0.35	49.0	-7	-15	-10
26834	05 39 38	-15 39.1	0.232	-0.106	67.0	G8	6.74	0.76	75.0	-43	-51	-16
49669	10 05 43	12 12.7	-0.254	0.006	5.9	B7 V	-0.68	-0.09	39.0	-27	-7	-13
55642	11 21 19	10 48.3	0.170	-0.075	-10.3	F2 IV	2.36	0.42	47.0	20	4	-6
57606	11 46 04	14 33.7	-0.110	0.000	3.0	F0 V	4.26	0.30	47.0	-10	-5	0
76267	15 32 34	26 52.9	0.136	-0.089	1.7	A0 V	0.39	-0.01	43.0	15	3	-7
81833	16 41 11	39 01.0	0.048	-0.082	8.3	G8 IV	2.11	0.92	53.0	10	5	2
93519	19 00 11	-00 47.1	0.031	-0.011	-26.0	G5	7.38	0.72	52.0	-22	-14	-2
98066	19 52 47	-26 26.0	0.231	0.083	-18.6	G3	3.40	0.75	55.0	-25	6	-5
98258	19 55 07	-15 37.5	0.017	-0.100	3.0	A2 V	3.32	0.05	46.0	4	-8	-6
105864	21 23 55	00 53.3	0.113	-0.163	11.0	F5 V	4.63	0.45	50.0	5	-4	-21
113136	22 51 60	-16 05.2	-0.041	-0.025	18.0	A3 V	1.24	0.07	39.0	11	5	-14

$\overline{v}_\phi$ is determined by asymmetric drift. Comparing stellar groups with small and large velocity dispersions gives a more accurate measurement of asymmetric drift. For this reason we divide the catalogue in samples (identified by a number k) according to the absolute magnitudes. The sample including the smallest absolute magnitude corresponds to the brightest stars or the bluest since all these stars are on the main sequence. This sample includes young stars and has their kinematic characteristic: low velocity dispersion. In contrast, samples with fainter stars have redder main sequence stars and are a mixture which includes older stars with higher velocity dispersion. We determine the sample division by minimizing the errors on the R_ρ and R_σ estimates.

Maximum likelihood is used to estimate the best model parameters. The likelihood function L is the product of likelihoods L_k, where L_k is the likelihood of sample number k.

$$L_k = \prod_{i=1,N_k} f_k(v_{R,i}, v_{\phi,i})/\Sigma_k \tag{11}$$

with

$$\Sigma_k = \int\int f_k dv_R dv_\phi \tag{12}$$

where N_k is the number of stars in sample k.

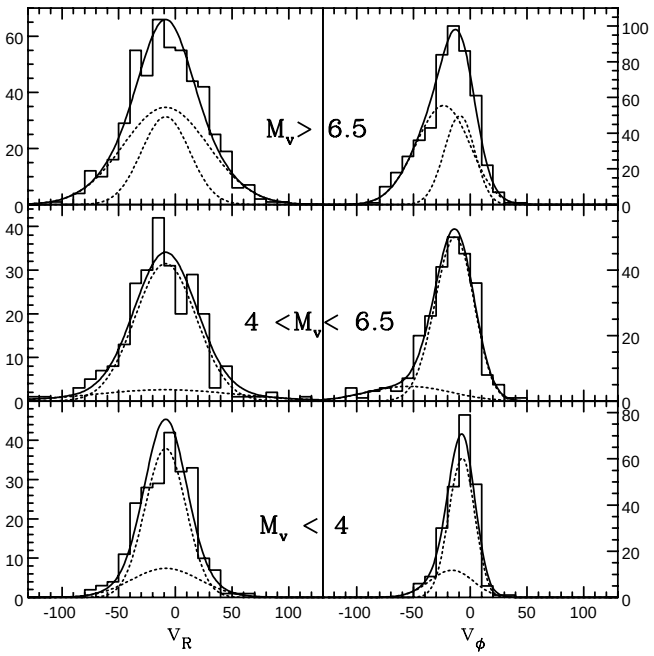

Fig. 3. Radial and tangential velocity histograms for three samples of stars sorted according to their absolute magnitude M_v. The maximum likelihood models are plotted (continuous lines) as well as individual DFs (dashed lines).

Each sample is modeled by using two elementary distribution functions, $f_k = f_{k,1} + f_{k,2}$ (continuous lines in Fig. 3) corresponding to the sum of two DFs (dashed lines in Fig. 3) given by Eqs. (1, 2, 7 and 8).

4.3. Results

Solutions do not depend significantly on the catalogues, the splitting method or the shape of the potentials considered (spherical, plane-parallel or intermediate). Best fits with the smallest errors are obtained using both catalogues simultaneously. Figure 3 shows the observed velocity histograms and the corresponding model curves for the best estimates of parameters with a plane-parallel potential and $R_0 = 8.5\,\mathrm{kpc}$ and $V_0 = 220\,\mathrm{km\ s^{-1}}$. This model is in good agreement with data (the reduced χ^2 is approximately one for each histogram).
The results obtained with each catalogue are given in Table 3 in case of plane-parallel models and in case of intermediate 3D models. $R_{\rho,eff}$ and $R_{\sigma,eff}$ scale lengths are the effective scale lengths of the computed density or dispersion that, in the case of high velocity dispersions, differ from the R_ρ or R_σ parameters used in Eqs. 3 and 4. Formal errors are small but we find a strong correlation of scale length with solar velocity $v_\odot$ which limits the accuracy of density scale length estimates and could bias our conclusions.

4.4. Sample splitting

We divided the stellar catalogue into one, two or three samples with various sizes and we made systematic explorations. We found subdivisions that minimize errors of non-local parameters. Within the error bars, other subdivisions gave solutions in agreement with the best fit. The best fit is obtained with two small samples with a low velocity dispersion and a large one with a high velocity dispersion. This corresponds certainly to the best way to constrain the asymmetric drift.

4.5. R_ρ and the solar velocity $v_\odot$

The maximum likelihood solution gives a small value of $R_{\rho,eff} = 1.7\,\mathrm{kpc}$. Plotting the asymmetric drift relation $v'_\odot = v_\odot + c < \Pi^2 >$ with the CNS3 catalogue yields a result different from Delhaye (1965) who obtained $v_\odot = 12\,\mathrm{km\ s^{-1}}$. It appears that the mean velocity v of the few tens of bluest CNS3 main sequence stars is small and favours a small $v_\odot$ value between 3 and $7\,\mathrm{km\ s^{-1}}$. This explains the small R_ρ found which is strongly correlated with $v_\odot$. Most recent $v_\odot$ determinations are small, Gómez and Mennessier (1977) found $6\,\mathrm{km\ s^{-1}}$, Mayor (1974) obtained $6.3\,\mathrm{km\ s^{-1}}$ and

Table 3. Model parameters: solar velocities, density and kinematic scale lengths, slope of the galactic velocity curve. Galactic structural parameters are obtained for various splittings of the data in absolute magnitude and assuming $R_0 = 8.5\,\mathrm{kpc}$ and $V_0 = 220\,\mathrm{km\ s^{-1}}$.

Catalogue	number of stars	splitting	$u_\odot$ km s^{-1}	$v_\odot$ km s^{-1}	$R_{\rho,eff}$ kpc	$R_{\sigma,eff}$ kpc	α
Plane-parallel models							
Reid et al.	477	1	8.4 ± 1.5	4.3 ± 4.4	1.9	36	$-.21 \pm .07$
Blue nearby stars	504	2 (228/276)	8.7 ± 1.1	2.5 ± 2.1	1.8	$24 - 30$	$-.23 \pm .06$
Reid and Blue stars	981	3 (228/256/497)	8.6 ± 0.9	2.2 ± 1.7	$1.7 \pm .3$	> 30	$-.22 \pm .05$
Reid and Blue stars with $R_0 = 7.9\,\mathrm{kpc}$, $V_0 = 185\,\mathrm{km\ s^{-1}}$	981	3 (228/256/497)	8.6 ± 0.9	2.6 ± 1.6	$2.0 \pm .3$	> 30	$-.18 \pm .04$
Reid and Blue stars : $\boldsymbol{v_\odot = 8}$	981	3 (228/256/497)	$8.7 \pm .9$	**8**	$2.9 \pm .3$	$18 - 30$	$-.20 \pm .05$
3D models							
Reid and Blue stars	981	3 (228/256/497)	8.5 ± 1.2	2.5 ± 2.2	$1.7 \pm .3$	> 30	$-.22 \pm .06$
Reid and Blue stars : $\boldsymbol{v_\odot = 8}$	981	3 (228/256/497)	8.6 ± 1.2	**8**	$2.8 \pm .4$	$20 - 30$	$-.20 \pm .06$

Delhaye (1982) found $8.5\,\mathrm{km\ s^{-1}}$. Some other references may be found in Kuijken and Tremaine (1991). Oblak (1983) built new samples carefully determining stellar ages in order to analyse the asymmetric drift. He found a small solar velocity $v_\odot = 5.0 \pm 0.7\,\mathrm{km\ s^{-1}}$.

To summarize, if we admit 2 and $8\,\mathrm{km\ s^{-1}}$ as the lower and upper limits on the $v_\odot$ solar velocity, we obtain limits on the effective density scale lengths $R_{\rho,eff}$ from 1.7 kpc to 2.9 kpc.

The scale length we have determined is proportional to the assumed solar galactic radius R_0; with our best fit it gives $R_\rho = 1.7 * (R_0/8.5)\,\mathrm{kpc}$.

5. Discussion and conclusion

Dynamical analysis of the stellar kinematics in our Galaxy is frequently based on the comparison between observed and modelled moments of the velocity and not directly on the measured distribution function. A practical reason for that is the apparent lack of simple dynamical models predicting realistic distribution functions. Moments contain most of the dynamical information. However their measurements based on observational data may be strongly biased by a few stars (high velocity members in a binary or halo stars when analyzing the disc). For example Cuddeford & Binney (1992) show how these biases can be reduced. Evans & Collett (1993) obtain new realistic DFs by generalising the Rybicki disc model, but in the case of exponential disk models with $R_\rho = R_{\sigma^2}$, they only obtain moments.

Here we have shown that *the Shu (1969) models that are exact solutions of the collisionless Boltzmann equation, can be used successfully to analyse galactic dynamics.* We build a nearly exponential stellar disc (much more accurately exponential than galactic discs really are), which includes the basic necessary parameters, the density and kinematic scale lengths, the slope of the rotation curve and which removes all restraining assumptions done in previous work. The comparison to the velocity distribution from an unbiased kinematic sample of nearby stars gives an accurate determination of the galactic structure: assuming $R_0 = 8.5\,\mathrm{kpc}$ and $V_0 = 220\,\mathrm{km\ s^{-1}}$, *we conclude that the stellar density scale length of the Milky Way ranges between 1.7 and 2.9* kpc. We obtain a large kinematic scale length; this is in poor agreement with the galactic R_σ determination obtained by Lewis and Freeman (1989) or by Bottema (1993) in external similar spiral galaxies. The large kinematic scale length that we find may result from the large proportion of young stars in our sample with a kinematic behaviour resembling gas that has a null kinematic gradient. It may result from the inadequacy of the model to also measure this parameter, e.g. if the accuracy of velocities in the Gliese catalogue is not sufficient. This could be checked swiftly with Hipparcos data. We find that *the rotation curve* $v_c(R) = R^\alpha$ *is decreasing at the solar galactic radius with* $\alpha = -0.22 \pm .05$. All these quantities are obtained from local stars that have non-negligible radial motions. It means that these structural parameters are mean values measured over an extent of a few kiloparsecs around the Sun. Mayor & Oblak (1985) and Oblak & Mayor (1987) proceed partly with a similar approach (maximum likelihood and Monte-Carlo) but based on numerical integration of stellar orbits in different galactic potentials. They find $R_{\sigma^2} = 5\,\mathrm{kpc}$ or $R_\sigma = 10\,\mathrm{kpc}$.

Few other previous kinematic determinations of the Galaxy scale lengths have been obtained assuming $R_\rho = R_{\sigma^2}$. Determinations were then obtained directly from the measurement of the kinematical scale length in the mid-plane, or from the asymmetric drift relation. Here the analysis of the local kinematics of stars shows that this assumption is wrong in the Galaxy and introduces bias favouring much larger estimates of R_ρ.

Recent analyses, using simpler distribution functions (Evans & Collett 1993 and Cuddeford & Binney 1992), one assuming $R_\rho = R_{\sigma^2}$ the other a flat rotation curve, were not able to reproduce accurately the observed DF. Our results are concordant with the work by Fux & Martinet (1994) based on Jeans equations expanded by Cuddeford & Amendt (1991) with assumptions to obtain the closure of the moment equations. They deduce a short density scale length and they conclude, as we do here, that this result does not support the assumption $\sigma_z(R)/\sigma_R(R) = const.$

The structural parameter values are obtained with a good accuracy. The small value of R_ρ obtained with our analysis of the kinematics of neighbouring stars is consistent with most recent determinations of the density: Robin et al. (1992ab) and Ojha et al. (1996) based on star counts or Durand et al. (1996) based on COBE maps. *We have shown that the hypothesis relating density and kinematic scale length $R_\rho = R_\sigma/2$ is incorrect* and that scale length determinations based on this assumption must be ruled out.

Acknowledgements. We would like to thank C. Lineweaver for his careful reading of the manuscript and L. Martinet for his valuable help to improve the paper.
This research has made use of the Simbad database, operated at CDS, Strasbourg, France.

References

Barbier-Brossat M., Petit M., Figon P., 1994, A&AS, 108, 603
Blitz L., Spergel D.N., 1991, ApJ, 370, 205
Bottema R., 1993, A&A, 275, 16
Burton W.B., te Lintel Hekkert P., 1986, A&AS, 65, 427
Cuddeford P., Amendt P., 1991, MNRAS, 253, 427
Cuddeford P., Binney J., 1994, MNRAS, 266, 273
Dambis A.K., Mel'nik A.M., Rastorguev A.S., 1995, Astronomy Letters Vol. 21 No 3, 291
Dehnen W., Binney J., 1995, "Formation of the Galactic Halo" Tucson, October 9-11, 1995 ASP Conference Series, eds Sarajedini A. & Morrison H.
de Jong R.S., 1996, A&A, 313, 377
Delhaye J., 1965, in Galactic Structure, Blaauw A., Schmidt M., eds, Univ. Chicago Press, Chicago, ch.4
Delhaye J., 1982, Mitteilungen der Astron. Gesellschaft, 57, 123
Durand S., Dejonghe H., Acker A., 1996, A&A, 310, 97
Elmegreen D.M., Elmegreen B.G., 1984, ApJS, 54, 127
Evans N.W., Collett J.L., 1993, MNRAS, 264, 353
Fich M., Blitz L., Stark A.A., 1989, ApJ, 342, 272
Fux R., Martinet L., 1994, A&A, 287, L21
Giovanardi C., Hunt L.K., 1988, AJ, 95, 408
Gliese W., Jahreiss H., 1991, Preliminary Version of the Third Catalogue of Nearby Stars, on The Astronomical Data Center CD-ROM: Selected Astronomical Catalogs, Vol. 1, eds. L. E. Brotzmann and S.E. Gesser, NASA/ADC, Greenbelt, MD
Gómez, A., Mennessier M.O., 1977, A&A, 54, 113
Haywood M., Robin A.C., Crézé M., 1996, A&A (in press)
Kent S.M., Dame T.M., Fazio G., 1991, ApJ 378, 131
Kerr F.J., Lynden-Bell D., 1986, MNRAS, 221, 1023
Kuijken K., Gilmore G., 1989, MNRAS, 239, 605
Kuijken K., Tremaine S., 1991, *Dynamics of Disk Galaxies*, Ed: B. Sundelius (Göteborg Univ. Press), 71
Kuijken K., Tremaine S., 1994, ApJ, 421, 178
Lewis J.R., Freeman K.C., 1989, AJ, 97, 139
Mayor M., 1974, A&A, 32, 321
Mayor M., Oblak E., 1985, The Milky Way Galaxy, Symp IAU 106, eds: H. van Woerden et al., 149
Neese C.L., Yoss K.M., 1988, AJ, 95, 463
Oblak E., 1983, A&A 123, 238
Oblak E., Mayor M., 1987, Evolution of Galaxies, X IAU European meeting, ed. J. Palous, Publ. Astron. Inst. Czech. Acad. Sci. 69, 263
Ojha D.K., Bienaymé O., Robin A.C., Crézé M., Mohan V., 1996, A&A 311, 456
Pont F., Mayor M., Burki G., 1994, A&A, 285, 415
Reid I.N., Hawley S. L., Gizis J.E., 1995, AJ, 110(4), 1838
Reid M.J., 1993, ARA&A, 31, 345
Robin A.C., Crézé M., Mohan V., 1992a, A&A, 265, 32
Robin A.C., Crézé M., Mohan V., 1992b, ApJ, 400, L25
Rohlfs K., Kreitschmann J., 1988, A&A, 201, 51
Shu F.H., 1969, ApJ, 158, 505
Statler T.S., 1989, ApJ 344, 217

Tamisier F., 1991, *Rapport de stage de DEA*, Observatoire de Paris
Turon C., Crézé M., Egret D. et al., 1992, The Hipparcos Input catalogue, Ed: ESA Publication division c/o ESTEC, Noordwijk
van Altena W.F., Lee J.T., Hoffleit D., 1991, The General Catalogue of Trigonometric Stellar Parallaxes, Preliminary Version (catalogue available at CDS: number I/174)
van der Kruit P.C., 1986, A&A, 157, 230

This article was processed by the author using Springer-Verlag LaTeX A&A style file *L-AA* version 3.